DOI: 10.1002/ejic.200700143

Synthesis and Spectro-electrochemical Aspects of $[\mathrm{Ru^{II}(trpy)(pdt)(X)}]^{n+}$ (trpy = 2,2′:6′,2′′-Terpyridine, pdt = 5,6-Diphenyl-3-pyridyl-*as*-triazine, X = $\mathrm{Cl^-}$, $\mathrm{CH_3CN}$, $\mathrm{NO_2^-}$, $\mathrm{NO^+}$, $\mathrm{NO^{\cdot}}$) – Electrophilicity of $\{\mathrm{Ru^{II}{-}NO^+}\}$ and Photolability of $\{\mathrm{Ru^{II}{-}NO^{\cdot}}\}$

Somnath Maji,[a] Chandrani Chatterjee,[a] Shaikh M. Mobin,[a] and Goutam Kumar Lahiri*[a]

Keywords: Ruthenium / Nitrosyl complexes / Spectroscopy / Electrochemistry / Reactivity

Nitrosylruthenium derivatives having $\mathrm{NO^+}$ and $\mathrm{NO^{\cdot}}$ states have been synthesized in a stepwise manner starting from $[\mathrm{Ru^{II}(trpy)(pdt)(Cl)}](\mathrm{ClO_4})$ $\{[\mathbf{1}](\mathrm{ClO_4})\}$ → $[\mathrm{Ru^{II}(trpy)(pdt)(CH_3CN)}](\mathrm{ClO_4})_2$ $\{[\mathbf{2}](\mathrm{ClO_4})_2\}$ → $[\mathrm{Ru^{II}(trpy)(pdt)(NO_2)}](\mathrm{ClO_4})$ $\{[\mathbf{3}](\mathrm{ClO_4})\}$ → $[\mathrm{Ru^{II}(trpy)(pdt)(NO^+)}](\mathrm{ClO_4})_3$ $\{[\mathbf{4}](\mathrm{ClO_4})_3\}$ → $[\mathrm{Ru^{II}(trpy)(pdt)(NO^{\cdot})}](\mathrm{ClO_4})_2$ $\{[\mathbf{4}](\mathrm{ClO_4})_2\}$ [trpy = 2,2′:6′,2′′-terpyridine, pdt = 5,6-diphenyl-3-pyridyl-*as*-triazine]. The molecular identity of $[\mathbf{1}](\mathrm{ClO_4})$ and $[\mathbf{2}](\mathrm{ClO_4})_2$ and the subsequent stereoretentive transformation of $[\mathbf{1}](\mathrm{ClO_4})$ → $[\mathbf{2}](\mathrm{ClO_4})_2$ have been authenticated by single-crystal X-ray structures. Electrochemical and spectral features are investigated as a function of the monodentate ligands ($\mathrm{Cl^-}$, $\mathrm{CH_3CN}$, $\mathrm{NO_2^-}$, $\mathrm{NO^+}$, $\mathrm{NO^{\cdot}}$). The kinetic and thermodynamic aspects of the reaction of the moderately strong electrophilic $\{\mathrm{Ru^{II}{-}NO^+}\}$ center [ν(NO): 1944 $\mathrm{cm^{-1}}$] in $[\mathbf{4}]^{3+}$ with a nucleophile such as $\mathrm{OH^-}$ have been studied. The nitrosyl species $[\mathrm{Ru^{II}(trpy)(pdt)(NO^+)}]^{3+}$ ($[\mathbf{4}]^{3+}$) can be selectively reduced to $[\mathrm{Ru^{II}(trpy)(pdt)(NO^{\cdot})}]^{2+}$ ($[\mathbf{4}]^{2+}$) electrochemically as well as chemically by hydrazine hydrate. On exposure to light an acetonitrile solution of $[\mathrm{Ru^{II}(trpy)(pdt)(NO^{\cdot})}]^{2+}$ ($[\mathbf{4}]^{2+}$) undergoes slow photocleavage of the $\mathrm{Ru^{II}{-}NO}$ bond over a period of 4 h, resulting in the corresponding solvated species $[\mathrm{Ru^{II}(trpy)(pdt)(CH_3CN)}]^{2+}$ ($[\mathbf{2}]^{2+}$). The rate of photolability of the $\mathrm{Ru^{II}{-}NO}$ bond in $[\mathbf{4}]^{2+}$ has been monitored spectrophotometrically.

Introduction

The biological[1] and environmental[2] relevance of the nitrosyl molecule has led to a resurgence of interest in the metal–NO interaction. This is primarily due to fundamental issues such as (i) bonding and redox features,[3] (ii) reactivity profile of metal-bound NO function with a variety of nucleophiles,[4] (iii) uses of nitrosylmetal derivatives as antitumor and antiseptic agents,[5] and (iv) photolytic cleavage of the M–NO bond and subsequent transfer of photoreleased "NO" to the biological targets such as myoglobin (Mb) or cytochrome c oxidase.[6]

The stability of possible redox states of the nitrosyl molecule, $\mathrm{NO^+}$, $\mathrm{NO^{\cdot}}$, and $\mathrm{NO^-}$, in the complex framework of (AL)M–NO depends on a variety of factors, including the nature of the metal ions and the ancillary ligands (AL). For example, in reduced vitamin $\mathrm{B_{12}}$, the cobalt center formally binds with the NO in the form of $\mathrm{Co^{III}{-}NO^-}$,[7] while in metmyoglobin the iron center binds with the NO formally as $\mathrm{Fe^{II}{-}NO^+}$.[8] Similarly, electrophilicity of the coordinated NO center in $\{\mathrm{(AL)(trpy)Ru^{II}{-}NO}\}$ (trpy = 2,2′:6′,2′′-terpyridine) can also be nicely tuned primarily depending on the electronic aspects of AL. Thus, the $\nu_{\mathrm{NO^+}}$ frequency as well as the $E°(\mathrm{NO^+/NO^{\cdot}})$ values systematically vary with AL = 2-phenylpyridine (pp),[9] acetylacetone (acac),[10] *N*-methyl-2-(2-pyridyl)benzimidazole (pNMebi),[11] (2-pyridyl)benzimidazole (pbi),[11] 2,2′-dipyridylamine (dpa),[12] bis(2-pyridyl) ketone (dpk),[13] 2,2′-bipyridine (bpy),[14] 2-(2-pyridyl)benzoxazole (pbo),[11] and 2-(phenylazo)pyridine (pap),[15] as shown in Table 1.

The observed distinct role of AL in the complex framework of $\{\mathrm{(AL)(trpy)Ru^{II}{-}NO^+}\}$ (Table 1) has initiated the selective introduction of 5,6-diphenyl-3-pyridyl-*as*-triazine (pdt) as AL to explore its specific effect towards the stability of coordinated NO in accessible redox states. The ligand pdt has been of interest in the field of coordination chemistry as well as organometallic chemistry since early 1964.[16] However, only a limited number of ruthenium complexes of pdt and its derivatives have been reported so far from different perspectives.[17]

The present article thus describes the stepwise synthetic aspects of the nitrosyl complexes starting from $[\mathrm{Ru^{II}(trpy)(pdt)(Cl)}](\mathrm{ClO_4})$ $\{[\mathbf{1}](\mathrm{ClO_4})\}$ → $[\mathrm{Ru^{II}(trpy)(pdt)(CH_3CN)}](\mathrm{ClO_4})_2$ $\{[\mathbf{2}](\mathrm{ClO_4})_2\}$ → $[\mathrm{Ru^{II}(trpy)(pdt)(NO_2)}](\mathrm{ClO_4})$ $\{[\mathbf{3}](\mathrm{ClO_4})\}$ → $[\mathrm{Ru^{II}(trpy)(pdt)(NO^+)}](\mathrm{ClO_4})_3$

---

[a] Department of Chemistry, Indian Institute of Technology-Bombay,
Powai, Mumbai 400076, India
E-mail: lahiri@chem.iitb.ac.in

Supporting information for this article is available on the WWW under http://www.eurjic.org or from the author.

Table 1. $\nu(NO^+)$ frequencies and reduction potentials of $\{Ru^{II}(NO^+)\} \rightarrow \{Ru^{II}(NO^\cdot)\}$ in $[Ru^{II}(trpy)(AL)(NO^+)]^{n+}$.

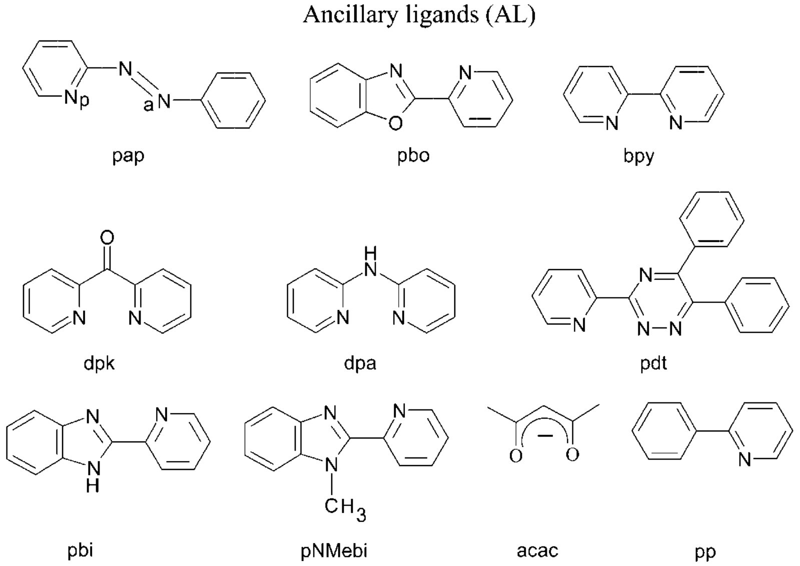

Ancillary ligand (AL)	$\nu(NO^+)$/cm^{-1}[a]	E°_{298}/V[b]	Ref.
pap	1960	0.72	[15]
pbo	1957	0.45	[11]
bpy	1952	0.45	[14]
dpk	1949	0.36	[13]
dpa	1945	0.34	[12]
pdt	1944	0.40	this work
pbi	1940	0.33	[11]
pNMebi	1932	0.31	[11]
acac	1914	0.02	[10]
pp	1858	–0.28	[9]

[a] In KBr disk. [b] CH_3CN/0.1 M Et_4NClO_4/SCE.

$\{[\mathbf{4}](ClO_4)_3\} \rightarrow [Ru^{II}(trpy)(pdt)(NO^\cdot)]^{2+}$ $\{[\mathbf{4}](ClO_4)_2\}$. Crystal structures of [**1**](ClO_4) and [**2**]$(ClO_4)_2$ and spectroelectrochemical features of all four complexes are reported. The reactivity of the ruthenium-bound electrophilic NO^+ in [**4**]$(ClO_4)_3$ in the presence of a nucleophile such as OH^- and the aspects of photolytic cleavage of the Ru^{II}–$NO^\cdot$ bond in $[\mathbf{4}]^{2+}$ are also investigated.

Results and Discussion

Synthesis and Characterization

The precursor chlorido complex $[Ru^{II}(trpy)(pdt)(Cl)]^+$ $[\mathbf{1}]^+$ [trpy = 2,2′:6′,2′′-terpyridine, pdt = 5,6-diphenyl-3-pyridyl-*as*-triazine] has been synthesized from $[Ru(trpy)Cl_3]$ and pdt in the presence of excess Et_3N and LiCl in refluxing EtOH. The crude product was subsequently purified by column chromatography on alumina. The product was isolated as its perchlorate salt [**1**](ClO_4). The solvated species [**2**]$(ClO_4)_2$ and the nitro derivative [**3**](ClO_4) were prepared from [**1**](ClO_4) and [**2**]$(ClO_4)_2$, respectively, as shown in Scheme 1. The desired nitroso complex $[Ru^{II}(trpy)(pdt)(NO^+)](ClO_4)_3$ $\{[\mathbf{4}](ClO_4)_3\}$ was prepared from the nitro derivative [**3**](ClO_4) by using concentrated nitric acid followed by concentrated perchloric acid at 273 K (Scheme 1).

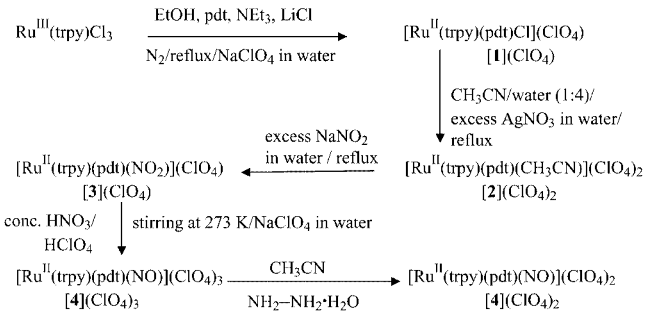

Scheme 1.

The direct synthesis of [**4**]$(ClO_4)_3$ either from the chlorido $\{[\mathbf{1}](ClO_4)\}$ or solvated $\{[\mathbf{2}](ClO_4)_2\}$ derivative using NO gas or $NOBF_4$ was not successful. Therefore, the stepwise synthetic route as shown in Scheme 1 was followed.

The diamagnetic complexes [**1**](ClO_4), [**2**]$(ClO_4)_2$, [**3**](ClO_4), and [**4**]$(ClO_4)_3$ exhibit expected molar conductivities and microanalytical data (see Experimental Section).

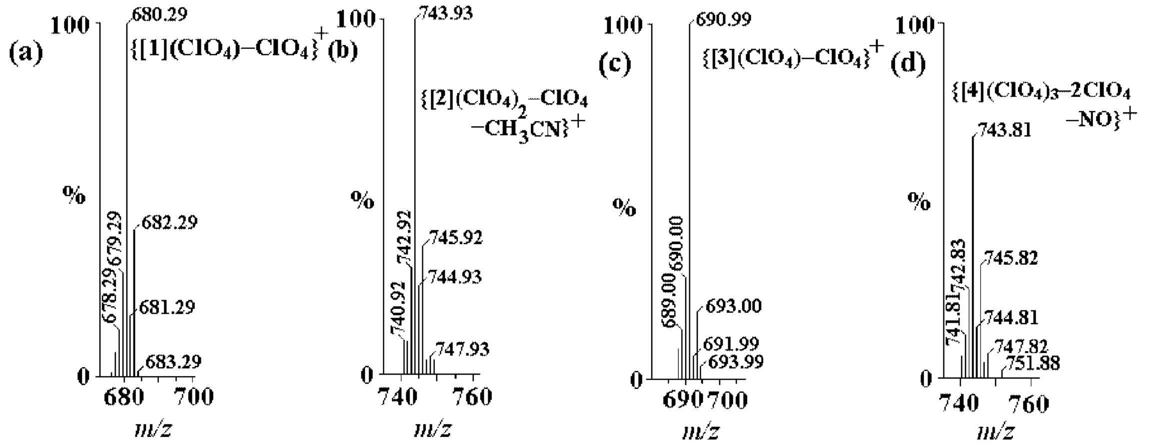

Figure 1. ESI mass spectra of (a) [**1**](ClO_4), (b) [**2**](ClO_4)$_2$, (c) [**3**](ClO_4), and (d) [**4**](ClO_4)$_3$ in CH_3CN.

The positive-ion electrospray mass spectra of [**1**](ClO_4), and [**3**](ClO_4) show molecular ion peaks centered at m/z = 680.29 and 690.99, respectively, corresponding to [**1**]$^+$ (calculated molecular mass: 680.09) and [**3**]$^+$ (calculated molecular mass: 690.11). Molecular ion peaks for [**2**](ClO_4)$_2$ and [**4**](ClO_4)$_3$ appear at m/z = 743.93 and 743.81 corresponding to {[**2**](ClO_4)$_2$ – ClO_4 – CH_3CN}$^+$ (calculated molecular mass: 744.07) and {[**4**](ClO_4)$_3$ – 2 ClO_4 – NO}$^+$ (calculated molecular mass: 744.15), respectively (Figure 1).

Orientation of the pyridyl or triazine ring of the unsymmetric pdt with respect to the monodentate ligand (X = Cl^- or CH_3CN or NO_2^- or NO) in the complex frameworks gives rise to two possible isomeric structures, **A** and **B**.

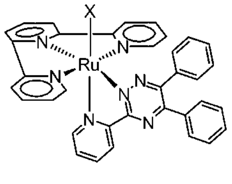

A

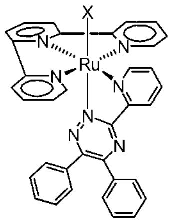

B

However, in practice, only one of the structural forms (**A** or **B**) has been systematically isolated by column chromatography for all the complexes. The preferential crystallization of isomer **A** where the pyridyl nitrogen atom is *trans* to "X" has been established by crystal structure analyses of [**1**](ClO_4) and [**2**](ClO_4)$_2$.

Crystal Structures of [1](ClO_4) and [2](ClO_4)$_2$·3H_2O

The crystal structures of [**1**](ClO_4) and [**2**](ClO_4)$_2$·3H_2O are shown in Figures 2 and 3, respectively. Selected crystallographic and structural parameters are listed in Tables 2 and 4, respectively.

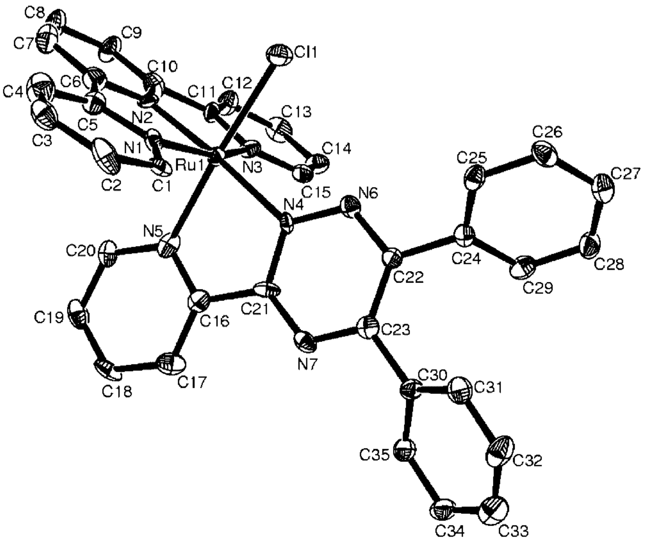

Figure 2. Crystal structure of the cation of [**1**](ClO_4).

The trpy ligand in the complexes is coordinated to the ruthenium ion in the expected meridional fashion with the bidentate pdt ligand in *cis* position. The intraligand *trans* angles, N1–Ru–N3 of 159.1(2) and 158.5(2)°, in [**1**](ClO_4) and [**2**](ClO_4)$_2$, respectively, reflect the usual geometrical constraints due to the meridional binding mode of tridentate trpy.[18] The other two interligand *trans* angles, N2–Ru–N4 and N5–Ru–X, remain close to 180° for both the complexes. As in other Ru–trpy derivatives,[18,19] the central Ru^{II}–N2(trpy) bonds {1.954(6) and 1.977(5) Å in [**1**](ClO_4) and [**2**](ClO_4)$_2$, respectively} are significantly shorter than the corresponding terminal Ru^{II}–N(trpy) distances, Ru–N1 [2.058(6) and 2.078(5) Å] and Ru^{II}–N3 [2.057(6) and 2.073(5) Å]. The pdt ligand forms a five-membered chelate ring to the metal ion through pyridyl and triazine nitrogen atoms. The coordinated pdt ligand is slightly nonplanar; the dihedral angles between the chelated pyridine and triazine

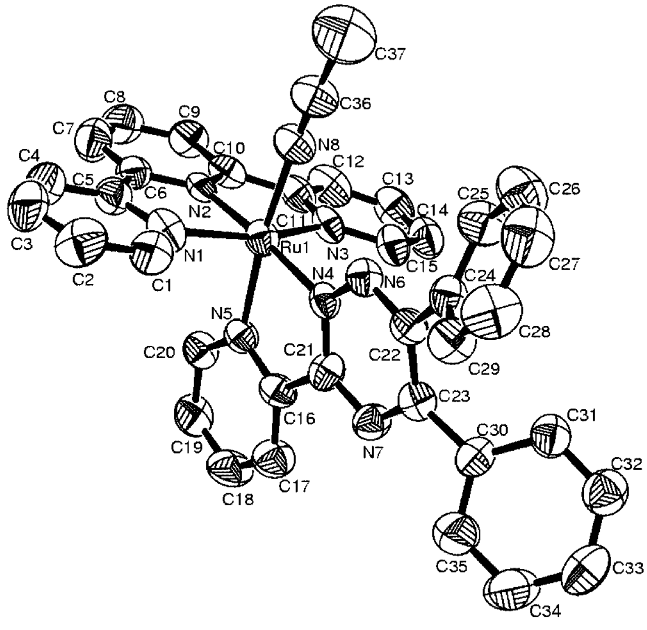

Figure 3. Crystal structure of the cation of [**2**]$(ClO_4)_2$. Water molecules of crystallization have been removed for clarity.

Table 2. Selected bond lengths [Å] and bond angles [°] for [**1**](ClO_4) and [**2**]$(ClO_4)_2\cdot3H_2O$.

	[**1**](ClO_4) (X = Cl)	[**2**]$(ClO_4)_2$ (X = CH_3CN)
Ru–X	2.392(2)	2.037(5)
Ru–N(1)	2.058(6)	2.078(5)
Ru–N(2)	1.954(6)	1.977(5)
Ru–N(3)	2.057(6)	2.073(5)
Ru–N(4)	2.042(6)	2.035(5)
Ru–N(5)	2.034(6)	2.047(4)
N(4)–N(6)	1.340(9)	1.355(6)
N(4)–C(21)	1.367(10)	1.348(7)
C(16)–C(21)	1.462(13)	1.471(9)
N(5)–C(16)	1.349(9)	1.347(7)
N(5)–C(20)	1.371(10)	1.356(7)
C(36)–N(8)	–	1.121(7)
N(1)–Ru–N(2)	79.7(2)	79.2(2)
N(1)–Ru–N(3)	159.1(2)	158.5(2)
N(1)–Ru–N(4)	100.6(2)	100.8(2)
N(1)–Ru–N(5)	87.0(2)	94.84(19)
N(2)–Ru–N(3)	79.4(2)	79.3(2)
N(2)–Ru–N(4)	175.5(3)	175.24(17)
N(2)–Ru–N(5)	96.9(2)	96.7(2)
N(3)–Ru–N(4)	100.3(2)	100.7(2)
N(3)–Ru–N(5)	96.6(2)	88.00(18)
N(4)–Ru–N(5)	78.6(2)	78.6(2)
N(1)–Ru–X	91.66(17)	87.4(2)
N(2)–Ru–X	87.91(18)	92.11(19)
N(3)–Ru–X	86.48(17)	93.00(19)
N(4)–Ru–X	96.55(17)	92.6(2)
N(5)–Ru–X	174.68(18)	171.2(2)
N(6)–N(4)–C(21)	119.2(6)	118.1(5)
N(4)–C(21)–C(16)	114.8(6)	114.6(6)
C(21)–C(16)–N(5)	114.0(7)	114.1(5)
C(16)–N(5)–C(20)	116.1(7)	116.8(5)
N(8)–C(36)–C(37)	–	177.8(9)

rings in [**1**](ClO_4) and [**2**]$(ClO_4)_2$ are 2.80(0.17) and 4.81(0.15)°, respectively. The dihedral angles between the pendant phenyl rings linked to the triazine ring are 52.13(0.26), 49.12(0.30) and 44.84(0.21), 55.09(0.25)° in [**1**](ClO_4) and [**2**]$(ClO_4)_2$, respectively. The Ru^{II}–Cl and Ru^{II}–N(pdt/trpy) bond lengths and the associated angles are in good agreement with the reported data on related molecules.[17a,18,19] The coordinated acetonitrile molecule in [**2**]$(ClO_4)_2$ is in its usual nearly linear mode with an N8–C36–C37 angle of 177.8(9)°.[13] The packing diagram of [**2**]$(ClO_4)_2\cdot3H_2O$ is shown in Figure S1 (Supporting Information).

^1H NMR, IR, UV/Vis and Emission Spectral Aspects

The ^1H NMR spectra of [**1**](ClO_4), [**2**]$(ClO_4)_2$, [**3**](ClO_4), and [**4**]$(ClO_4)_3$ in $(CD_3)_2SO$ are shown in Figure S2 (Supporting Information and Experimental Section). The complexes display 25 severely overlapping signals in the aromatic region between δ = 7.0 and 9.0 ppm. This matches well with the calculated number of aromatic signals, 11 and 14 resonances from the trpy and pdt ligands, respectively.

The ClO_4^- vibrations are observed at 1096/623, 1089/625, 1097/623, and 1087/626 cm^{-1} for [**1**](ClO_4), [**2**]$(ClO_4)_2$, [**3**](ClO_4), and [**4**]$(ClO_4)_3$, respectively. Ru^{II}–NO_2 stretching frequencies of [**3**](ClO_4) fall at 1366 cm^{-1} (asym.) and 1276 cm^{-1} (sym.). The ν_{NO^+} stretching frequency of 1944 cm^{-1} for [**4**]$(ClO_4)_3$ (Figure 4) is comparable to that reported for analogous complexes with AL = pbi, dpa or dpk (Table 1). However, it is much lower than that reported for AL = strongly π-acidic pap, pbo or bpy and much higher with respect to AL = strongly σ-donating pp, acac or pNMebi (Table 1). Thus, the observed reasonably high ν_{NO} stretching frequency of [**4**]$(ClO_4)_3$ is suggestive of its moderate electrophilic character.

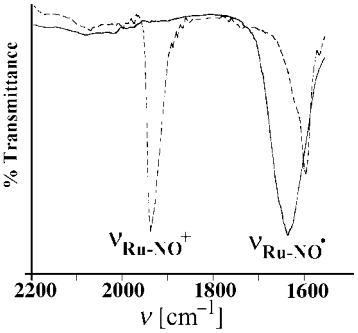

Figure 4. IR spectra (KBr disk) of (a) [**4**]$(ClO_4)_3$ (------) and (b) [**4**]$(ClO_4)_2$ (—) in the region of 2200–1600 cm^{-1}.

The complexes exhibit multiple transitions in the UV/Vis region in CH_3CN (Figure 5, Table 3). Intense ligand-based transitions (π → π* and n → π*) are observed in the UV region. The ruthenium(II)-based moderately intense metal-to-ligand charge-transfer (MLCT) transitions appear near 500 nm. The Gaussian analysis of the visible region of the spectra reveals the presence of two close bands in each of $[1]^+$, $[2]^{2+}$, and $[3]^+$ (Table 3 and inset of Figure 5).

These are tentatively assigned to $d\pi(Ru^{II}) \rightarrow \pi^*$(pdt)- and $d\pi(Ru^{II}) \rightarrow \pi^*$(trpy)-based transitions.[13,17] The MLCT band energy in acetonitrile solution follows the or-

Table 3. Redox potentials[a,b] and electronic spectroscopic data.

Compound	Couple				λ/nm
	I	II	III	IV	(ε/M^{-1} cm^{-1})[d]
[**1**]ClO$_4$	0.89(90)	–1.07(120)	–1.54(190)	–	520 (15073), [522 (4668), 506 (13100)[e]], 312 (38078), 279 (38762), 236 (33057), 204 (65481)
[**2**](ClO$_4$)$_2$	1.33(80)	–1.04(100)	–1.50(90)	–	470 (13942), [471 (6518), 448 (9499)[e]], 327 (23247),[f] 297 (38484), 202 (67952)
[**3**]ClO$_4$	1.09(90)	–1.05(80)	–1.54(110)	–	482 (11273), [479 (6952), 465 (4192)[e]], 297 (31685), 205(63910)
[**4**](ClO$_4$)$_3$	0.40(110)	–0.33[c]	–0.90(50)	–1.11(120)	467 (15528), [470 (4728), 451 (10036)[e]], 335 (27408),[f] 300 (40440), 207 (70624)
[**4**](ClO$_4$)$_2$					494 (15536), [505 (5350), 484 (13214)[e]], 307 (37634), 281 (36672), 272 (36284)

[a] Potentials $E°_{298}$/V (ΔE/mV) vs. SCE. [b] In CH_3CN/0.1 M Et_4NClO_4. [c] E_{pc} is considered due to the irreversible nature of the wave. [d] In acetonitrile. [e] Bands obtained by Gaussian analysis of the lowest energy transition. [f] Shoulder.

der Cl^- (520 nm) < NO_2^- (482 nm) < CH_3CN (470 nm) < NO^+ (467 nm) depending on the relative stabilization of the dπ(Ru^{II}) level.[20] The tripositive charge as well as pronounced π-acceptor characteristics of NO^+ in [**4**]$^{3+}$ are indeed reflected in the relatively higher MLCT band energy and the corresponding redox processes (see later). The 15-nm (666 cm^{-1}) blueshift in the MLCT band energy while moving from Ru^{II}–NO_2^- [**3**](ClO$_4$) (482 nm) to Ru^{II}–NO$^+$ [**4**](ClO$_4$)$_3$ (467 nm) is much less than that observed for analogous complexes having π-acidic ancillary ligands (dpk, bpy, pap).[13–15] This implies relatively weaker dπRu^{II} → π∗(NO$^+$) backbonding in [**4**](ClO$_4$)$_3$, as is also been evidenced in the ν(NO$^+$) stretching frequency (Table 1).

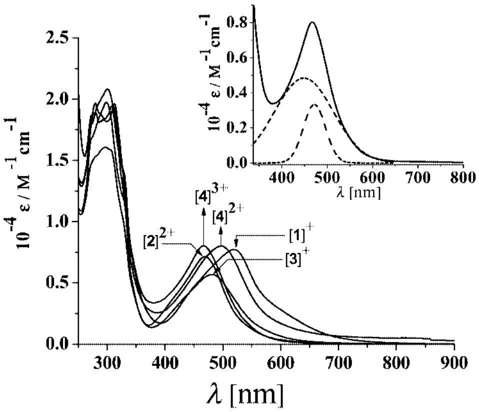

Figure 5. Electronic spectra in acetonitrile of [**1**]$^+$, [**2**]$^{2+}$, [**3**]$^+$, [**4**]$^{3+}$, and [**4**]$^{2+}$. Inset shows the Gaussian analysis (------) of the experimental spectrum (—) of [**2**]$^{2+}$ in the visible region.

Though excitations of [**1**]$^+$, [**3**]$^+$, and [**4**]$^{3+}$ at the lowest energy MLCT bands failed to show emissions even in EtOH/MeOH (4:1) glass (77 K), [**2**]$^{2+}$ exhibits weak emission at 640 nm (Figure S3, Supporting Information). The quantum yield, &πηι; = 0.026, was calculated with reference to Ru(bpy)$_3^{2+}$ (&πηι; = 0.34).[21] The observed emission of [**2**]$^{2+}$ can be attributed to the triplet MLCT state.[22]

Rates and Equilibrium Constant for the Conversion of [Ru^{II}(trpy)(pdt)(NO$^+$)]$^{3+}$ [4]$^{3+}$ → [Ru^{II}(trpy)(pdt)(NO$_2$)]$^+$ [3]$^+$

Unlike earlier reported analogous nitrosyl complexes,[11–13,15] [**4**]$^{3+}$ is found to be quite stable both in the solid state as well as in CH_3CN or even in poorly soluble water medium, in spite of the reasonably high ν(NO$^+$) stretching frequency of 1944 cm^{-1}. However, in the presence of a strong nucleophile such as OH$^-$, it undergoes slow transformation to the corresponding nitro derivative ([**3**]$^+$) [Equation (1)] (Figure 6). On the other hand, for the aforesaid analogous complexes, a weak nucleophile such as H_2O was found to be effective to perform the reaction stated in Equation (1).

$$\underset{[4]^{3+}}{[Ru^{II}(trpy)(pdt)(NO^{-})]^{3+}} + OH^- \rightarrow \underset{[3]^{+}}{[Ru^{II}(trpy)(pdt)(NO_2)]^{+}} + H^+ \quad (1)$$

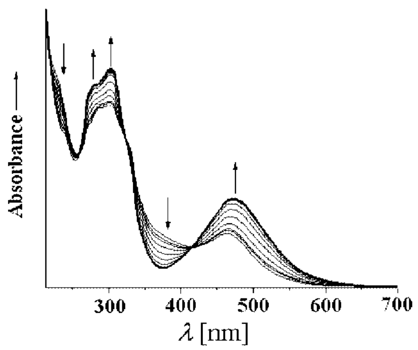

Figure 6. Time evolution of the electronic spectra (5-min time interval) of a changing solution of [Ru^{II}(trpy)(pdt)(NO$^+$)]$^{3+}$ (0.4 × 10^{-4} M) + OH$^-$ (0.1 × 10^{-2} M) → [Ru^{II}(trpy)(pdt)(NO$_2$)]$^+$ + H$^+$ in CH_3CN at 318 K. Arrows indicate increase or decrease in absorbances with the progression of the reaction.

The rate of conversion of the nitroso derivative ([**4**]$^{3+}$, 0.4 × 10^{-4} M) to the nitro counterpart ([**3**]$^+$) was monitored spectrophotometrically in the temperature range of 298–

318 K in CH_3CN solvent using a calculated optimum concentration of aqueous NaOH solution (0.1×10^{-2} M). CH_3CN was chosen as a solvent because of the poor solubility of $[\mathbf{4}]^{3+}$ in H_2O and thus the transformation process was monitored without any pH control. The well-defined isosbestic points (Figure 6) imply the involvement of nitrosyl and nitro species as the primary components in the conversion process. The pseudo-first-order rate constant (k/s), activation parameters ($\Delta H^{\#}/\Delta S^{\#}$), and equilibrium constant (K) values are calculated to be: 4.13×10^{-4} (298 K), 7.30×10^{-4} (308 K), 1.29×10^{-3} (318 K); 42.26 kJ mol^{-1}/–110.48 J K^{-1} mol^{-1}; 6.6, respectively. The observed appreciably large negative $\Delta S^{\#}$ value confirms that the nucleophilic attack of the electrophilic NO^+ site in $[\mathbf{4}]^{3+}$ by OH^- occurs through an associatively activated process. The equilibrium constant value of 6.6 indicates the presence of an appreciable concentration of the initial nitrosyl species $[Ru^{II}(trpy)(pdt)(NO^+)]^{3+}$ ($[\mathbf{4}]^{3+}$) in the equilibrated situation even under strongly alkaline condition.

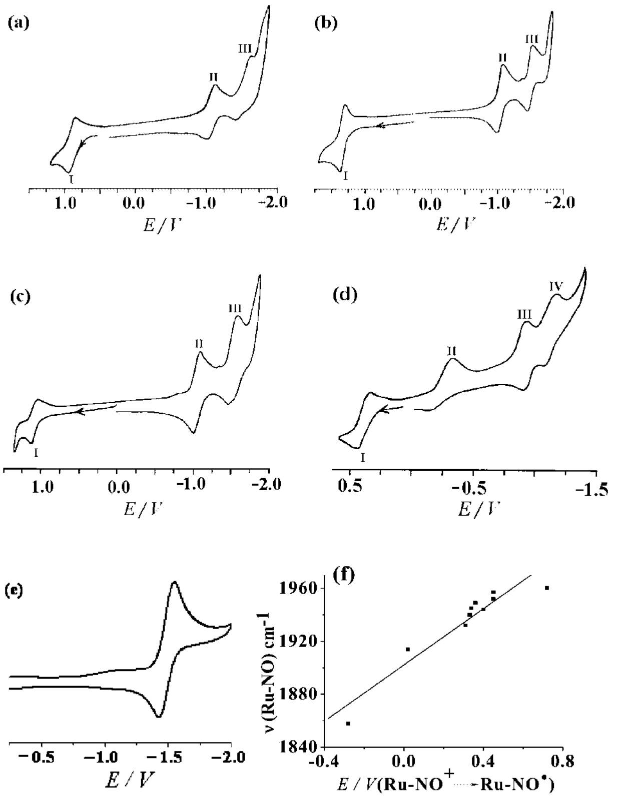

Figure 7. Cyclic voltammograms of (a) $[\mathbf{1}]^+$, (b) $[\mathbf{2}]^{2+}$, (c) $[\mathbf{3}]^+$, (d) $[\mathbf{4}]^{3+}$, (e) free ligand, pdt in CH_3CN (scan rate: 50 mV s^{-1}), and (f) least-squares plot of E/V (Ru^{II}–NO^+–Ru^{II}–$NO^{\cdot}$) vs. ν(Ru^{II}–NO^+) frequency of $[Ru^{II}(trpy)(AL)(NO^+)]^{3+}$ complexes where AL = pap, bpy, pbo, pdt, dpk, dpa, pbi, pNMebi, acac, and pp as listed in Table 1.

Redox and Spectroelectrochemical Aspects

The Ru^{III}/Ru^{II} potentials of $[\mathbf{1}]^+$, $[\mathbf{2}]^{2+}$, and $[\mathbf{3}]^+$ (couple I, Figure 7a–c; Table 3) vary depending on the electron-donating/-withdrawing nature of the monodentate ligand (X) as well as the electrostatic factor because of the overall charge of the complex moieties. They follow the expected trend of X = Cl^- (0.89) < NO_2^- (1.09) << CH_3CN (1.33 vs. SCE). The potentials are comparable to those of the corresponding $[Ru^{II}(trpy)(AL)(X)]^{n+}$, where AL = dpk,[13] having a π-conjugated electron-withdrawing C=O function (X = Cl^-, 0.88; NO_2^-, 1.02 V; CH_3CN, 1.37 V vs. SCE). However, the potentials are much higher than those of the analogous AL = dpa[12] derivatives incorporating a π-donor amine group (X = Cl^-, 0.64; NO_2^-, 0.88 vs. SCE). The two ligand-based reductions are observed in the range of –1.0 to –1.5 V (couples II and III, Figure 7a–c, Table 3). The first reduction wave near –1.0 V appears to be less than that typical for the trpy-based reductions (–1.30 and –1.80 V) observed in numerous Ru–trpy complexes.[18–20,23] On the other hand, the free pdt ligand reduces reversibly, $E°_{298}$/V (ΔE/mV) at –1.49 (120) versus SCE in CH_3CN (Figure 7e). Thus, couples II and III are assigned as the reduction processes involving pdt and trpy ligands, respectively.

The nitrosyl complex $[\mathbf{4}]^{3+}$ exhibits four successive reduction processes (couples I–IV, Figure 7d, Table 3). The effects of neutrality as well as low basicity of both the pdt and trpy ligands and the highly charged feature of $[\mathbf{4}]^{3+}$ facilitate the reversible reduction at the rather positive potential of 0.40 V versus SCE in CH_3CN (couple 1, Figure 7d). The same effect has also been extended even for the second one-electron reduction of $[\mathbf{4}]^{3+}$ (couple II, Figure 7d) at a reasonably less negative potential of –0.33 V, though irreversible at the cyclic voltammetric timescale. The potentials of couples I and II are much more positive relative to the reductions involving the coordinated pdt and trpy ligands, –0.90 and –1.11 V (couples III and IV, Figure 7d). Therefore, couples I and II are logically considered as the expected successive reductions of the redox facile coordinated NO^+, that is, $\{Ru^{II}–NO^+\} \rightarrow \{Ru^{II}–NO^{\cdot}\}$ and $\{Ru^{II}–NO^{\cdot}\} \rightarrow \{Ru^{II}–NO^-\}$, respectively. The difference in potential of 0.73 V (couple II/couple I) between the successive NO-centered reductions leads to a large comproportionation constant (K_c) value of $10^{12.4}$ ($RT\ln K_c = \Delta E/0.059$)[24] for the intermediate $\{Ru^{II}–NO^{\cdot}\}$ radical species $[\mathbf{4}]^{2+}$. The $Ru^{II}–NO^+ \rightarrow Ru^{II}–NO^{\cdot}$ reduction potentials and the corresponding $\nu(NO^+)$ values for the analogous $[Ru^{II}(trpy)(AL)(NO^+)]^{3+}$ complexes with AL = pap,[15] bpy,[14] pbo,[11] dpk,[13] dpa,[12] pbi,[11] pNMebi,[11] acac,[10] and pp[9] (Table 1) follow a general trend. Consequently, the plot of $E_{1/2}$ of the $Ru^{II}–NO^+/Ru^{II}–NO^{\cdot}$ couple versus the $\nu(NO^+)$ frequency for the known $[Ru^{II}(trpy)(AL)(NO^+)]^{3+}$ derivatives yields a reasonably linear relationship (Figure 7f).

Nitrosyl species $[\mathbf{4}]^{3+}$ can be quantitatively reduced to $[\mathbf{4}]^{2+}$ either coulometrically or by using hydrazine hydrate as a chemical reducing agent. The relevant microanalytical, conductivity, and mass spectrometric data are given in the Experimental Section. On reduction of $[\mathbf{4}]^{3+}$ to $[\mathbf{4}]^{2+}$, the ν(NO) frequency is shifted from 1944 to 1633 cm^{-1} (Figure 4) The large $\Delta\nu$ value of 311 cm^{-1} on moving from $[\mathbf{4}]^{3+}$ to $[\mathbf{4}]^{2+}$ confirms[25] the reduction of coordinated NO^+ to

NO$^{\cdot}$. Consequently, the reduced species $[\mathbf{4}]^{2+}$ exhibits a radical-type EPR spectrum (g = 2.003) with partially resolved nitrogen hyperfine splittings.[11–13,26] On reduction to the nitrosyl radical complex $[\mathbf{4}]^{2+}$, the visible-energy charge-transfer band has been reasonably redshifted from 467 to 494 nm (Figure 5). Moreover, two distinct bands involving the singly occupied MO appear at 307 and 281 nm[13] (Figure 5, Table 3). However, the second reduced species $[\mathbf{4}]^{+}$ with the NO^{-} state was found to be unstable even on the coulometric timescale at 298 K.

Photocleavage of the Ru^{II}–NO Bond in [Ru^{II}(trpy)(pdt)(NO$^{\cdot}$)]$^{2+}$ ([4]$^{2+}$)

Though $[\mathbf{4}]^{2+}$ is quite stable in CH_3CN under ambient light conditions, exposure of an acetonitrile solution of $[\mathbf{4}]^{2+}$ to light (Xenon 350 W lamp) for a period of about 4 h results in quantitative transformation to the solvated species $[\mathbf{2}]^{2+}$ by the selective cleavage of the Ru^{II}–NO$^{\cdot}$ bond. The slow but steady progression of photocleavage of the Ru^{II}–NO$^{\cdot}$ bond of $[\mathbf{4}]^{2+}$ was monitored spectrophotometrically in CH_3CN (Figure 8) and the presence of isosbesticities suggests the clean conversion of [Ru^{II}(trpy)(pdt)(NO$^{\cdot}$)]$^{2+}$ ($[\mathbf{4}]^{2+}$) to [Ru^{II}(trpy)(pdt)(CH_3CN)]$^{2+}$ ($[\mathbf{2}]^{2+}$). The rate of first-order photolytic release of NO (k_{NO}) has been determined to be 4.4×10^{-3} min^{-1} ($t_{1/2}\approx 157$ min). This sort of photolytic cleavage of the M–NO bond maintaining the overall integrity of the rest of the molecule is known to have biological relevance.[6] However, because of the insolubility of $[\mathbf{4}]^{2+}$ in aqueous medium, it has not been possible so far to explore the feasibility of transferring the photoliberated NO to biomolecules such as myoglobin or cytochrome c oxidase. Thus, further work in the direction of developing newer classes of water-soluble nitrosyl derivatives is in progress.

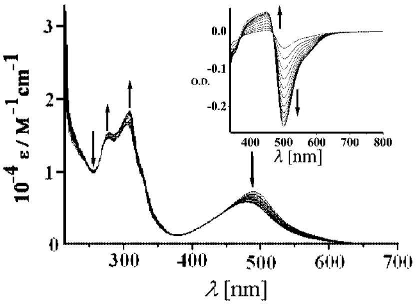

Figure 8. Time evolution of the electronic spectra (20-min time interval) of a changing solution of [Ru^{II}(trpy)(pdt)(NO$^{\cdot}$)]$^{2+}$ ($\mathbf{4}^{2+}$, 0.4×10^{-4} M) in CH_3CN exposed to light (Xe lamp 350 W). Arrows indicate increase or decrease in absorbances with the progression of the reaction. The inset shows the difference spectra of $\mathbf{4}^{2+}$ exposed to light (Xe lamp 350 W) at different time intervals with respect to unexposed $[\mathbf{4}]^{2+}$ in acetonitrile as the reference solution.

Conclusions

The present work demonstrates the substitutional and electron-transfer aspects of a series of four compounds based on the framework of [Ru^{II}(trpy)(pdt)X]$^{n+}$ {X = Cl^{-} ($[\mathbf{1}]^{+}$), CH_3CN ($[\mathbf{2}]^{2+}$), NO_2^{-} ($[\mathbf{3}]^{+}$), NO^{+} ($[\mathbf{4}]^{3+}$)}. The nitrosyl function in $[\mathbf{4}]^{3+}$ undergoes facile two-step one-electron reductions: {Ru^{II}–NO^{+}} to {Ru^{II}–NO$^{\cdot}$} to {Ru^{II}–NO^{-}}. Unlike earlier reported analogous complexes {[Ru^{II}(trpy)(AL)(NO^{+})]$^{n+}$} with AL = pap, pbo, bpy, dpk, dpa, pbi, pNMebi, $[\mathbf{4}]^{3+}$ is found to be sufficiently stable both in the solid and solution (CH_3CN or poorly in water medium) states in spite of the moderately strong electrophilic character of the nitrosyl function [ν(Ru^{II}–NO^{+}) = 1944 cm^{-1}]. $[\mathbf{4}]^{3+}$ transforms slowly and partially to the corresponding nitro derivative $[\mathbf{3}]^{+}$ only in the presence a of strongly alkaline medium. The NO^{+} function in [Ru^{II}(trpy)(pdt)(NO^{+})]$^{3+}$ ($[\mathbf{4}]^{3+}$) can be quantitatively reduced to the corresponding NO$^{\cdot}$ state in [Ru^{II}(trpy)(pdt)(NO$^{\cdot}$)]$^{2+}$ ($[\mathbf{4}]^{2+}$) either electrochemically or chemically by using hydrazine hydrate. Though $[\mathbf{4}]^{2+}$ is stable under ambient light conditions, the exposure of an acetonitrile solution of $[\mathbf{4}]^{2+}$ to light (Xenon 350 W lamp) for a period of 4 h results in the solvated species $[\mathbf{2}]^{2+}$ by the slow photorelease of NO with k_{NO} of 4.4×10^{-3} min^{-1} ($t_{1/2}\approx 157$ min).

Experimental Section

Materials and Instrumentation: The precursor complexes Ru^{III}(trpy)Cl_3[27] and 5,6-diphenyl-3-pyridyl-*as*-triazine (pdt)[28] were prepared according to reported procedures. 2,2′:6′,2′′-Terpyridine, 2-cyanopyridine, and silver nitrate were purchased from Aldrich. Other chemicals and solvents were reagent-grade and used as received. For spectroscopic studies, HPLC-grade solvents were used. Solution electrical conductivity was checked using a Systronic conductivity bridge 305. Infrared spectra were taken with a Nicolet spectrophotometer with samples prepared as KBr pellets. ^{1}H NMR spectra were recorded with a 300-MHz Varian FT spectrometer with $(CD_3)_2SO$ used as solvent. Cyclic voltammetric and coulometric measurements were carried out using a PAR model 273A electrochemistry system. A platinum wire working electrode, a platinum wire auxiliary electrode, and a saturated calomel reference electrode (SCE) were used in a standard three-electrode configuration. Tetraethylammonium perchlorate (TEAP) was used as the supporting electrolyte and the solution concentration was about 10^{-3} M; the scan rate used was 50 mV s^{-1}. A platinum gauze working electrode was used in the coulometric experiments. All electrochemical experiments were carried out under dinitrogen. UV/Vis spectral studies were performed with a Perkin–Elmer Lambda 950 spectrophotometer. The elemental analyses were carried out with a Perkin–Elmer 240C elemental analyzer. Electrospray mass spectra were recorded with a Micromass Q-ToF mass spectrometer. Steady-state emission experiments were performed using a Perkin–Elmer LS 55 luminescence spectrometer fitted with a cryostat.

Synthesis of [Ru^{II}(trpy)(pdt)(Cl)]ClO$_4$ {[1](ClO$_4$)}: [Ru^{III}(trpy)Cl_3] (100 mg, 0.23 mmol) was dissolved in ethanol (20 mL) and 5,6-diphenyl-3-pyridyl-*as*-triazine (pdt) (41.8 mg, 0.227 mmol), excess LiCl (54 mg, 1.3 mmol), and NEt_3 (0.4 mL) were added to it. The mixture was heated at reflux under dinitrogen for 5 h. The initial dark brown solution gradually changed to deep purple. The dry mass thus obtained on removal of solvent under reduced pressure was dissolved in a minimum volume of acetonitrile, and excess saturated aqueous solution of $NaClO_4$ was added to it. The resulted solid precipitate was filtered off and washed thoroughly with cold water. The product was dried in vacuo over P_4O_{10}. It was then purified on a neutral alumina column. The complex [**1**](ClO_4) was eluted with CH_2Cl_2/CH_3CN (3:1). Evaporation of the solvents under reduced pressure afforded pure complex [**1**](ClO_4). Yield: 113.2 mg (64 %). $C_{35}H_{25}Cl_2N_7O_4Ru$ (779.04): calcd. C 53.91, H 3.23, N 12.58; found C 54.27, H 3.08, N 12.27. Molar conductivity in acetonitrile: Λ_M = 127 Ω^{-1} cm^2 M^{-1}. ^{1}H NMR [300 MHz, $(CD_3)_2SO$, 298 K]: δ = 8.87 (d, J = 8.1 Hz, 1 H), 8.75 (d, J = 8.1 Hz, 2 H), 8.65 (d, J = 8.1 Hz, 1 H), 8.45 (d, J = 8.1 Hz, 1 H), 8.27 (m, 2 H), 8.03 (t, J = 8.1, 6.9 Hz, 3 H), 7.77 (d, J = 4.8 Hz, 2 H), 7.59 (m, 3 H), 7.42 (m, 7 H), 7.23 (t, J = 7.8, 7.5 Hz, 1 H), 7.05 (1 H), 6.94 (d, J = 7.2 Hz, 1 H) ppm.

Synthesis of [Ru^{II}(trpy)(pdt)(CH_3CN)](ClO_4)$_2$ {[2](ClO_4)$_2$}: The chlorido complex [**1**](ClO_4) (100 mg, 0.128 mmol) was dissolved in CH_3CN (5 mL), water (20 mL) was added and then the mixture was heated at reflux for 10 min. An excess of $AgNO_3$ (217 mg, 1.28 mmol) was added to the above hot solution and the heating was continued for a further 2 h. The solution was then cooled and the precipitated AgCl was separated by filtration through a sintered glass crucible (G-4). On concentration of the filtrate, the desired solid complex [**2**](ClO_4)$_2$ separated. It was filtered and washed with ice-cold water and subsequently dried in vacuo over P_4O_{10}. Yield: 90.8 mg (80 %). $C_{37}H_{28}Cl_2N_8O_8Ru$ (884.04): calcd. C 50.22, H 3.19, N 12.67; found C 49.99, H 3.13, N 12.45. Molar conductivity (CH_3CN): Λ_M = 270 Ω^{-1} cm^2 M^{-1}. ^{1}H NMR [300 MHz, $(CD_3)_2SO$, 298 K]: δ = 8.99 (d, J = 8.1 Hz, 2 H), 8.83 (t, J = 6.6, 7.8 Hz, 3 H), 8.72 (d, J = 7.8 Hz, 1 H), 8.55 (t, J = 7.8, 8.1 Hz, 1 H), 8.27 (d, J = 4.8 Hz, 1 H), 8.16 (t, J = 7.5, 7.8 Hz, 2 H), 8.07 (t, J = 7.5, 6.6 Hz, 1 H), 7.91 (m, 2 H), 7.79 (d, J = 2.1 Hz,1 H), 7.53 (m, 9 H), 7.25 (t, J = 8.1, 7.5 Hz, 1 H), 6.92 (d, J = 7.2 Hz, 1 H) ppm.

Synthesis of [Ru^{II}(trpy)(pdt)(NO_2)](ClO_4) [3](ClO_4): The complex [**2**](ClO_4)$_2$ (100 mg, 0.116 mmol) was dissolved in CH_3CN (5 mL) and then water (20 mL) was added followed by an excess of $NaNO_2$ (200 mg, 2.90 mmol). The mixture was heated at reflux for 2.5 h. The deep red solution of [**2**](ClO_4)$_2$ changed to deep orange during the course of the reaction. The pure crystalline nitro complex precipitated when the hot solution cooled to room temperature. The solid [**3**](ClO_4) thus obtained was filtered off, washed with ice-cold water, and dried in vacuo over P_4O_{10}. Yield: 73.3 mg (82 %). $C_{35}H_{25}ClN_8O_6Ru$ (790.06): calcd. C 53.20, H 3.19, N 14.18; found C 53.37, H 3.26, N 13.94. Molar conductivity in acetonitrile: Λ_M = 120 Ω^{-1} cm^2 M^{-1}. ^{1}H NMR [300 MHz, $(CD_3)_2SO$, 298 K]: δ = 8.99 (d, J = 8.1 Hz, 1 H), 8.85 (m, 2 H), 8.75 (m, 2 H), 8.27 (d, J = 5.1 Hz,1 H), 8.17 (t, J = 6.3, 8.7 Hz, 1 H), 8.05 (m, 2 H), 7.90 (m, 2 H), 7.75 (m, 2 H), 7.49 (m, 10 H), 7.24 (t, J = 7.5, 7.8 Hz, 1 H), 6.95 (d, J = 7.5 Hz, 1 H) ppm.

Synthesis of [Ru^{II}(trpy)(pdt)(NO^+)](ClO_4)$_3$ {[4](ClO_4)$_3$}: Dropwise addition of concentrated HNO_3 (2 mL) to the powdered nitro complex [**3**](ClO_4) (100 mg, 0.126 mmol) at 273 K whilst stirring resulted in a pasty mass. The pasty mass thus formed was added to ice-cold concentrated $HClO_4$ (6 mL) dropwise with continuous stirring using a glass rod. On further addition of saturated aqueous $NaClO_4$ solution, a yellow solid product formed. The precipitate was filtered off immediately, washed with a little ice-cold water and then dried in vacuo over P_4O_{10}. Yield: 98.3 mg (80 %). $C_{35}H_{25}Cl_3N_8O_{13}Ru$ (971.96): calcd. C 43.20, H 2.59, N 11.52; found C 43.02, H 2.46, N 11.74. Molar conductivity (CH_3CN): Λ_M = 310 Ω^{-1} cm^2 M^{-1}. ^{1}H NMR [300 MHz, $(CD_3)_2SO$, 298 K]: δ = 9.20 (m, 1 H), 9.08 (d, J = 3.9 Hz, 1 H), 8.96 (m, 1 H), 8.83 (t, J = 7.5, 7.8 Hz, 1 H), 8.57 (m, 3 H), 8.27 (d, J = 5.1 Hz, 1 H), 8.19 (m, 2 H), 8.05 (m, 1 H), 7.88 (m, 3 H), 7.51 (m, 9 H), 6.97 (t, J = 7.1, 6.9 Hz, 1 H), 6.85 (d, J = 7.5 Hz, 1 H) ppm.

Synthesis of [Ru^{II}(trpy)(pdt)($NO^{\cdot}$)](ClO_4)$_2$ {[4](ClO_4)$_2$}: The nitroso complex [**4**](ClO_4)$_3$ (100 mg, 0.102 mmol) was dissolved in 5 mL of CH_3CN and excess hydrazine hydrate was added whilst stirring over a period of 5 min. The stirring was continued for a further 1 h. The initial yellow solution of [**4**](ClO_4)$_3$ changed to red-brown. The solvent was then removed under reduced pressure and the solid mass thus obtained was washed with a little ice-cold water and then dried in vacuo over P_4O_{10}. Yield: 67.4 mg (75 %). $C_{35}H_{25}Cl_2N_8O_9Ru$ (873.02): calcd. C 48.11, H 2.89, N 12.83; found C 47.92, H 2.86, N 12.98. Molar conductivity (CH_3CN): Λ_M = 225 Ω^{-1} cm^{-2} M^{-1}. Magnetic moment (298 K): μ_B = 1.87. MS: *m/z* = calcd. for {[**4**](ClO_4)$_2$ – ClO_4 – NO} 744.15, found 744.31.

CAUTION! *Perchlorate salts of metal complexes with organic ligands are potentially explosive. Heating of dried samples must be avoided and handling of small amounts has to proceed with great caution, using protection.*

Kinetic Experiments: For the determination of k of the conversion process of [Ru^{II}(trpy)(pdt)(NO^+)]$^{3+}$ ([**4**]$^{3+}$) $\rightarrow$ [Ru^{II}(trpy)(pdt)(NO_2)]$^+$ ([**3**]$^+$) in acetonitrile in the presence of aqueous sodium hydroxide solution, the increase in absorbance (A_t) at 482 nm corresponding to λ_{max} of the nitro complex was recorded as a function of time (t). $A\alpha$ was measured when the intensity changes leveled off. Values of pseudo-first-order rate constants, k, were obtained from the slopes of linear least-squares plots of $-\ln(A\alpha - A_t)$ against t. The activation parameters $\Delta H^{\#}$ and $\Delta S^{\#}$ were determined from the Eyring plot.[29] The first-order rate constant for the photo release of NO from [**4**]$^{2+}$ was determined from the single-exponential fitting of the plot of Δ(OD) against time, where Δ(OD) is the differential absorbance at 494 nm of [**4**]$^{2+}$ in acetonitrile, exposed to light, with respect to unexposed [**4**]$^{2+}$ in acetonitrile as the reference solution.

X-ray Crystallography: Single crystals of [**1**](ClO_4) or [**2**](ClO_4)$_2$ were grown by slow diffusion of an acetonitrile solution of the complex into toluene, followed by slow concentration. X-ray data were collected using an Oxford Xcalibur-S CCD single-crystal X-ray diffractometer using Mo-K_α radiation. Crystal data and data collection parameters are listed in Table 4. The structures were solved and refined by full-matrix least squares on F^2 using SHELX-97 (SHELXTL).[30] Absorption corrections for [**1**](ClO_4) and [**2**](ClO_4)$_2$ were performed by multiscan. All the data were corrected

Table 4. Crystallographic data for [**1**](ClO_4) and [**2**](ClO_4)$_2$·3H_2O.

	[**1**](ClO_4)	[**2**](ClO_4)$_2$
Empirical formula	$C_{35}H_{25}Cl_2N_7O_4Ru$	$C_{37}H_{28}Cl_2N_8O_{11}Ru$
Formula mass	779.59	932.64
Crystal symmetry	monoclinic	monoclinic
Space group	*P*21	*P*21/*a*
a/Å	8.485(3)	19.612(5)
b/Å	14.4596(8)	8.6085(10)
c/Å	13.368(3)	25.267(6)
α/°	90.0	90.0
β/°	102.89(3)	108.21(2)
γ/°	90.0	90.0
V/Å^3	1598.7(7)	4052.2(14)
Z	2	4
μ/mm^{-1}	0.711	0.588
T/K	100(2)	293(2)
$D_{calcd.}$/g cm^{-3}	1.602	1.529
F (000)	788	1888
2θ range/°	5.92–50.0	6.32–57.20
e data (R_{int})	5164 (0.0438)	8003 (0.0605)
R_1, wR_2 [$I > 2\sigma(I)$]	0.0505, 0.1152	0.0687, 0.1426
R_1, wR_2 (all data)	0.0629, 0.1193	0.1657, 0.1670
Gof	1.042	0.885
Largest diff. peak/hole/e Å^{-3}	2.354/–0.486	0.607/–0.596

for Lorentz and polarization effects, and the non-hydrogen atoms were refined anisotropically. Hydrogen atoms were included in the refinement process as per the riding model. X-ray analysis revealed the presence of three water molecules as solvent of crystallization in $[\mathbf{2}](\mathrm{ClO}_4)_2$. CCDC-635850 {for $[\mathbf{1}](\mathrm{ClO}_4)$} and -635851 {for $[\mathbf{2}](\mathrm{ClO}_4)_2$} contain the supplementary crystallographic data for this paper. These data can be obtained free of charge from The Cambridge Crystallographic Data Centre via www.ccdc.cam.ac.uk/data_request/cif.

Supporting Information (see footnote on the first page of this article): Packing diagram of $[\mathbf{2}](\mathrm{ClO}_4)_2\cdot 3\mathrm{H}_2\mathrm{O}$ along the *b* axis (Figure S1), ^{1}H NMR spectra of (a) $[\mathbf{1}]^+$, (b) $[\mathbf{2}]^{2+}$, (c) $[\mathbf{3}]^+$, and (d) $[\mathbf{4}]^{3+}$ in $(\mathrm{CD}_3)_2\mathrm{SO}$ (Figure S2), and emission spectrum of $[\mathbf{2}]^{2+}$ in EtOH/MeOH (4:1) glass at 77 K (Figure S3).

Acknowledgments

Financial support received from the Department of Science and Technology and Council of Scientific and Industrial Research, New Delhi, India is gratefully acknowledged. X-ray structural studies for $[\mathbf{1}](\mathrm{ClO}_4)$ and $[\mathbf{2}](\mathrm{ClO}_4)_2$ were carried out at the National Single Crystal Diffractometer Facility, Indian Institute of Technology, Bombay. Special acknowledgment is made to the Sophisticated Analytical Instrument Facility (SAIF) for providing the NMR and EPR facilities.

[1] a) J. B. Howard, D. C. Rees, *Chem. Rev.* **1996**, *96*, 2965; b) B. K. Burgees, D. J. Lowe, *Chem. Rev.* **1996**, *96*, 2983; c) R. R. Eady, *Chem. Rev.* **1996**, *96*, 3013; d) J. S. Stamler, D. J. Singel, J. Loscalzo, *Science* **1992**, *258*, 1898; e) E. Culotta Jr, D. E. Koshland, *Science* **1992**, *258*, 1862; f) S. Pfeiffer, B. Mayer, B. Hemmens, *Angew. Chem. Int. Ed.* **1999**, *38*, 1714; g) G. B. Richter-Addo, P. Legzdins, J. Burstyn, *Chem. Rev.* **2002**, *102*, 857; h) S. Moncada, R. M. J. Palmer, E. A. Higgs, *Pharmacol. Rev.* **1991**, *43*, 109; i) G. B. Ritcher-Addo, P. Legzdins in *Metal Nitrosyls*, Oxford University Press, New York, **1992**; j) W. R. Scheidt, M. K. Ellison, *Acc. Chem. Res.* **1999**, *32*, 350; k) K. Karidi, A. Garoufis, A. Tsipis, N. Hadjiliadis, H. D. Dulk, J. Reedijk, *Dalton Trans.* **2005**, 1176; l) N. Bettache, T. Carter, J. E. T. Corrie, D. Ogden, D. R. Trentham in *Methods in Enzymology* (Ed.: L. Packer), Academic Press, San Diego, CA, **1996**, vol. 268, p. 266; m) D. R. Lang, J. A. Davis, L. G. F. Lopes, A. A. Ferro, L. C. G. Vasconcellos, D. W. Franco, E. Tfouni, A. Wieraszko, M. J. Clarke, *Inorg. Chem.* **2000**, *39*, 2294; n) P. C. Ford, J. Bourassa, K. Miranda, B. Lee, I. Lorkovic, S. Boggs, S. Kudo, L. Laverman, *Coord. Chem. Rev.* **1998**, *171*, 185; o) E. Tfouni, M. Krieger, B. R. McGarvey, D. W. Franco, *Coord. Chem. Rev.* **2003**, *236*, 57; p) A. Franke, N. Hessenauer-Ilicheva, D. Meyer, G. Stochel, W. D. Woggon, R. van Eldik, *J. Am. Chem. Soc.* **2006**, *128*, 13611; q) R. K. Afshar, A. A. Eroy-Reveles, M. M. Olmstead, P. K. Mascharak, *Inorg. Chem.* **2006**, *45*, 10347.

[2] a) K. K. Pandey, *Coord. Chem. Rev.* **1983**, *51*, 69; b) V. Zang, R. van Eldik, *Inorg. Chem.* **1990**, *29*, 4462; c) E. K. Pham, S. G. Chang, *Nature* **1994**, *369*, 139.

[3] a) M. Videla, J. S. Jacinto, R. Baggio, M. T. Garland, P. Singh, W. Kaim, L. D. Slep, J. A. Olabe, *Inorg. Chem.* **2006**, *45*, 8608; b) P. Singh, B. Sarkar, M. Sieger, M. Niemeyer, J. Fiedler, S. Zalis, W. Kaim, *Inorg. Chem.* **2006**, *45*, 4602; c) M. Sieger, B. Sarkar, S. Zalis, J. Fiedler, N. Escola, F. Doctorovich, J. A. Olabe, W. Kaim, *Dalton Trans.* **2004**, 1797.

[4] a) J. A. McCleverty, *Chem. Rev.* **1979**, *79*, 53; b) A. Das, C. J. Jones, J. A. McCleverty, *Polyhedron* **1993**, *12*, 327; c) M. H. Thiemens, W. C. Trogler, *Science* **1991**, *251*, 932; d) M. Feelisch, J. S. Stamler (Eds.), *Methods in Nitric Oxide Research*, Wiley, Chichester, England, **1996**; e) J. H. Enemark, R. D. Felthan, *Coord. Chem. Rev.* **1974**, *13*, 339; f) F. Bottomley in *Reactions of Coordinated Ligands* (Ed.: P. S. Braterman), Plenum, New York, **1985**, vol. 2, p. 115; g) P. C. Ford, I. M. Lorkovic, *Chem. Rev.* **2002**, *102*, 993; h) F. Bottomley, *Acc. Chem. Res.* **1978**, *11*, 158; i) F. Roncaroli, M. E. Ruggiero, D. W. Franco, G. L. Estiu, J. A. Olabe, *Inorg. Chem.* **2002**, *41*, 5760.

[5] a) S. P. Fricker, E. Slade, N. A. Powell, O. J. Vaughn, G. R. Henderson, S. A. Murrer, I. C. Megson, S. K. Bisland, F. W. Flitney, *Br. J. Pharmacol.* **1997**, *122*, 1441; b) N. Bettache, T. Carter, J. E. T. Corrie, D. Ogden, D. R. Trentham in *Methods in Enzymology* (Ed.: L. Packer), Academic Press, San Diego, CA, **1996**, Vol. 268, p. 266; c) N. Davies, M. T. Wilson, E. Slade, S. P. Fricker, B. A. Murrer, N. A. Powell, G. R. Henderson, *Chem. Commun.* **1997**, 47; d) Y. Chen, R. E. Shepherd, *J. Inorg. Biochem.* **1997**, *68*, 183; e) J. M. Slocik, M. S. Ward, R. E. Shepherd, *Inorg. Chim. Acta* **2001**, *317*, 290; f) L. G. F. Lopes, A. Wieraszko, Y. El-Sherif, M. J. Clarke, *Inorg. Chim. Acta* **2001**, *312*, 15; g) C. W. B. Bezerra, S. C. Silva, M. T. P. Gambardella, R. H. A. Santos, L. M. A. Plicas, E. Tfouni, D. W. Franco, *Inorg. Chem.* **1999**, *38*, 5660; h) J. W.-S. Hui, W.-T. Wong, *Coord. Chem. Rev.* **1998**, *172*, 389; i) S.-M. Lee, W.-T. Wong, *Coord. Chem. Rev.* **1997**, *164*, 415.

[6] a) A. K. Patra, P. K. Mascharak, *Inorg. Chem.* **2003**, *42*, 7363; b) B. O. Fernandez, I. M. Lorkovic, P. C. Ford, *Inorg. Chem.* **2004**, *43*, 5393.

[7] M. Wolak, G. Stochel, A. Zahl, T. Schneppensieper, R. van Eldik, *J. Am. Chem. Soc.* **2001**, *123*, 9780.

[8] L. E. Laverman, A. Wanat, J. Oszajca, G. Stochel, P. C. Ford, R. van Eldik, *J. Am. Chem. Soc.* **2001**, *123*, 285.

[9] H. Hadadzadeh, M. C. DeRosa, G. P. A. Yap, A. R. Rezvani, R. J. Crutchley, *Inorg. Chem.* **2002**, *41*, 6521.

[10] A. Dovletoglou, S. A. Adeyemi, T. J. Meyer, *Inorg. Chem.* **1996**, *35*, 4120.

[11] N. Chanda, D. Paul, S. Kar, S. M. Mobin, A. Datta, V. G. Puranik, K. K. Rao, G. K. Lahiri, *Inorg. Chem.* **2005**, *44*, 3499.

[12] N. Chanda, S. M. Mobin, V. G. Puranik, A. Datta, M. Niemeyer, G. K. Lahiri, *Inorg. Chem.* **2004**, *43*, 1056.

[13] S. Sarkar, B. Sarkar, N. Chanda, S. Kar, S. M. Mobin, J. Feidler, W. Kaim, G. K. Lahiri, *Inorg. Chem.* **2005**, *44*, 6092.

[14] D. W. Pipes, T. J. Meyer, *Inorg. Chem.* **1984**, *23*, 2466.

[15] B. Mondal, H. Paul, V. G. Puranik, G. K. Lahiri, *J. Chem. Soc., Dalton Trans.* **2001**, 481.

[16] a) A. A. Soudi, F. Marandi, A. Morsali, R. Kempe, I. Hortle, *J. Coord. Chem.* **2005**, *58*, 1631; b) W. Xiang-Li, *J. Inorg. Biochem.* **2004**, *98*, 1143; c) M. Koerner, P. A. Tregloan, R. van Eldik, *Dalton Trans.* **2003**, 2710; d) S. Das, B. K. Panda, *Polyhedron* **2006**, *25*, 2289; e) C. W. Jiang, *Eur. J. Inorg. Chem.* **2004**, *11*, 2217; f) R. Hege, J. G. Haasnoot, J. Reedijk, *Inorg. Chim. Acta* **1990**, *172*, 19.

[17] a) H. Deng, J. Li, K. C. Zheng, Y. Yang, H. Chao, L. N. Li, *Inorg. Chim. Acta* **2005**, *358*, 3430; b) C. W. Jiang, *Inorg. Chim. Acta* **2005**, *358*, 1231; c) C. W. Jiang, *Inorg. Chim. Acta* **2004**, *357*, 3403; d) C. W. Jiang, *J. Inorg. Biochem.* **2004**, *98*, 497; e) C. W. Jiang, H. Chao, X. L. Hong, H. Li, W. J. Mei, L. N. Ji, *Inorg. Chem. Commun.* **2003**, *6*, 773; f) H. Chao, G. Yang, G. Q. Xue, H. Li, H. Zang, I. D. Williams, L. N. Ji, X. M. Chen, X. Y. Li, *J. Chem. Soc., Dalton Trans.* **2001**, 1326; g) X. L. Hong, H. Chao, J. H. Yao, H. Li, L. N. Ji, *Polyhedron* **2004**, *23*, 815.

[18] a) B. Mondal, V. G. Puranik, G. K. Lahiri, *Inorg. Chem.* **2002**, *41*, 5831; b) N. Chanda, B. Mondal, V. G. Puranik, G. K. Lahiri, *Polyhedron* **2002**, *21*, 2033; c) V. J. Catalano, R. A. Heck, A. Ohman, M. G. Hill, *Polyhedron* **2000**, *19*, 1049; d) V. J. Catalano, R. A. Heck, C. E. Immoos, A. Ohman, M. G. Hill, *Inorg. Chem.* **1998**, *37*, 2150.

[19] S. Patra, B. Sarkar, S. Ghumaan, M. P. Patil, S. M. Mobin, R. B. Sunoj, W. Kaim, G. K. Lahiri, *Dalton Trans.* **2005**, 1188.

[20] B. Mondal, M. G. Walawalkar, G. K. Lahiri, *J. Chem. Soc., Dalton Trans.* **2000**, 4209.

[21] a) R. Alsfasser, R. van Eldik, *Inorg. Chem.* **1996**, *35*, 628; b) P. Chen, R. Duesing, D. K. Graff, T. J. Meyer, *J. Phys. Chem.* **1991**, *95*, 5850.

[22] a) S. Kar, N. Chanda, S. M. Mobin, A. Datta, F. A. Urbanos, V. G. Puranik, R. Jimenez-Aparicio, G. K. Lahiri, *Inorg. Chem.* **2004**, *43*, 4911; b) B. Sarkar, R. H. Laye, B. Mondal, S. Chakraborty, R. L. Paul, J. C. Jeffery, V. G. Puranik, M. D. Ward, G. K. Lahiri, *J. Chem. Soc., Dalton Trans.* **2002**, 2097; c) A. Juris, V. Balzani, F. Barigelletti, S. Campagna, P. Belser, A. Von Zelewsky, *Coord. Chem. Rev.* **1988**, *84*, 85.

[23] a) T. B. Hedda, H. L. Bozec, *Inorg. Chim. Acta* **1993**, *204*, 103; b) G. B. Deacon, J. M. Patrick, B. W. Skelton, N. C. Thomas, A. H. White, *Aust. J. Chem.* **1984**, *37*, 929.

[24] C. Creutz, *Prog. Inorg. Chem.* **1983**, *30*, 1.

[25] M. Wanner, T. Scheiring, W. Kaim, L. D. Slep, L. M. Baraldo, J. A. Olabe, S. Zalis, E. J. Baerends, *Inorg. Chem.* **2001**, *40*, 5704.

[26] a) V. R. de Souza, A. M. da Costa Ferreira, H. E. Toma, *Dalton Trans.* **2003**, 458; b) B. R. McGarvey, A. A. Ferro, E. Tfouni, C. W. D. Bezerra, I. A. Bagatin, D. W. Franco, *Inorg. Chem.* **2000**, *39*, 3577; c) R. W. Callahan, T. J. Meyer, *Inorg. Chem.* **1977**, *16*, 574; d) P. Diversi, M. Fontani, M. Fuligni, F. Laschi, F. Marchetti, S. Matteoni, C. Pinzino, P. Zanello, *J. Organomet. Chem.* **2003**, *675*, 21.

[27] M. T. Indelli, C. A. Bignozzi, F. Scandola, J.-P. Collin, *Inorg. Chem.* **1998**, *37*, 6084.

[28] F. H. Case, *J. Org. Chem.* **1965**, *30*, 931.

[29] R. G. Wilkins, *The Study of Kinetics and Mechanism of Reaction of Transition Metal Complexes*, Allyn and Bacon, Boston, MA, **1974**.

[30] G. M. Sheldrick, *Program for Crystal Structure Solution and Refinement*, Universität Göttingen, Göttingen, Germany, **1997**.

Received: January 31, 2007